Available online at www.sciencedirect.com
ScienceDirect
Quaternary International 161 (2007) 67–76

Sources and modes of terrigenous sediment input to the Chilean continental slope

Jan-Berend W. Stuut[a,*], Sabine Kasten[a,b], Frank Lamy[c], Dierk Hebbeln[a]

[a]*Research Center Ocean Margins (RCOM), P.O. Box 330440, 28334 Bremen, Germany*
[b]*Alfred Wegener Institute for Polar and Marine Research (AWI), Am Handelshafen 12, 27570 Bremerhaven, Germany*
[c]*GeoForschungsZentrum (GFZ) Potsdam, Telegrafenberg C 320, 14473 Potsdam Germany*

Available online 20 December 2006

Abstract

Physical, chemical, and mineralogical properties of a set of surface sediment samples collected along the Chilean continental slope (21–44°S) are used to characterise present-day sedimentation patterns and sediment provenance on the Chilean margin. Despite the presence of several exceptional latitudinal gradients in relief, oceanography, tectonic evolution, volcanic activity and onshore geology, the present-day input of terrigenous sediments to the Chilean continental margin appears to be mainly controlled by precipitation gradients, and source–rock composition in the hinterland. General trends in grain size denote a southward decrease in median grain-size of the terrigenous ($C_{organic}$, $CaCO_3$ and Opal-free) fraction, which is interpreted as a shift from aeolian to fluvial sedimentation. This interpretation is supported by previous observations of southward increasing bulk sedimentation rates. North–south trends in sediment bulk chemistry are best recognised in the iron (Fe) and titanium (Ti) vs. potassium (K) and aluminium (Al) ratios of the sediments that most likely reflect the contribution of source rocks from the Andean volcanic arc. These ratios are high in the northernmost part, abruptly decrease at ~25°S, and then more or less constantly increase southwards to a maximum at ~40°S.

1. Introduction

The Chilean margin provides a 'natural laboratory' for the analysis of sedimentation processes and sediment budgets due to its extraordinary latitudinal gradients in environmental and geological settings such as topography, climate, tectonics, volcanic activity, oceanography, and onshore geology. North to south changes in topography are obvious from the comparison of latitudinal elevation transects from the coast (or even from the Peru–Chile trench) towards the high Andes. Highest elevation contrasts are found in the northern part of Chile, where the Andes reach elevations of up to 7000 m asl. In combination with the Peru–Chile trench caused by the subduction of the Nazca plate underneath the South American one, this leads to spectacular topographic differences of up to ~15 km that gradually decrease southwards (Fig. 1). Based on these exceptional topographic contrasts, one would expect comparably extreme large denudation rates and, as a consequence, high sediment supply to the continental margin off northern Chile. However, the lack of any significant precipitation (see below) strongly limits denudation rates within the Atacama Desert. In contrast, erosion appears to be much stronger in the humid mountains in southern Chile although topographic gradients are smaller there (Scholl et al., 1970) (Fig. 1).

The regional geology of Chile is very complex. The underlying subduction geometry strongly influences topography and volcanism in the Andes that define the present-day volcanic arc (e.g., Ruiz and Corvalan, 1968; Zeil, 1986; Thornburg and Kulm, 1987a; Jordan and Gardeweg, 1989; Allmendinger et al., 1997; Sernageomin, 2003; Stern, 2004). The second important physiographic unit of Chile is the Coastal Range (indicated in Fig. 1), which is separated from the Andes by a longitudinal depression zone forming the Chilean Central Depression south of 33°S, and by several alluvial basins, especially north of 27.5°S. In this northern area, the Coastal Range exhibits an abrupt morphologic rise from sea level to

*Corresponding author.
E-mail address: jbstuut@rcom-bremen.de (J.-B. Stuut).

1040-6182/$ - see front matter © 2006 Elsevier Ltd and INQUA. All rights reserved.
doi:10.1016/j.quaint.2006.10.041

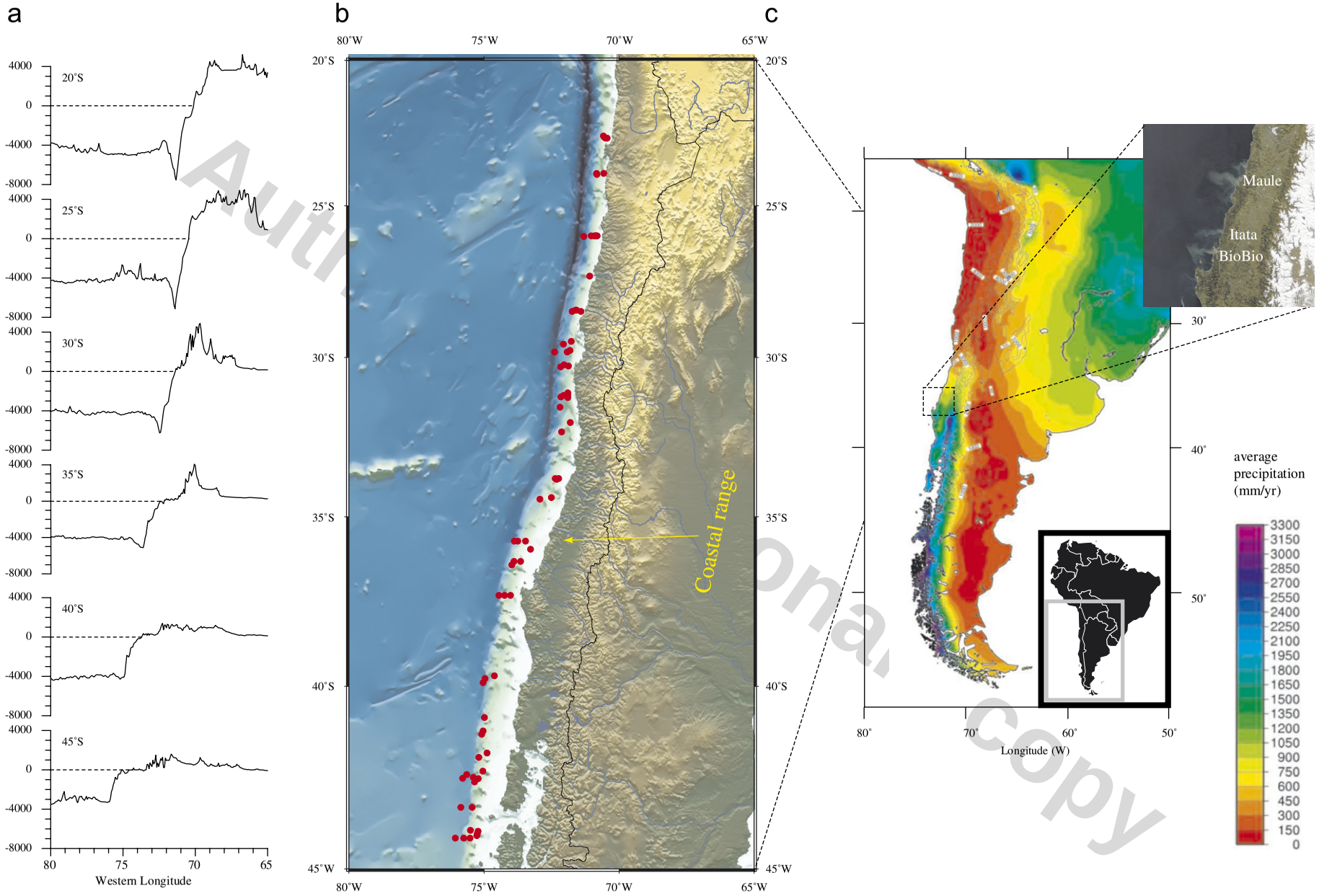

Fig. 1. Topographic map of western South America and bathymetry of the southeastern Pacific Ocean: (a) west–east topographic transects are shown at 5° latitude intervals to demonstrate the spectacular geomorphologic gradients in the study area, (b) Locations of surface sediment samples ($N = 70$) are indicated on the elevation map with red dots, (c) Zonation of rainfall ranging from hyperarid in the North to very humid in the South (after New et al., 2001). Insert: satellite image demonstrating fluvial input of sediments to the Pacific Ocean. These sediment plumes originate from the Maule, Itata and BioBio Rivers. From NASA's earthobservatory website, © Orbital Imaging Corporation and processing by NASA Goddard Space Flight Center.

elevations of 2000–2500 m. It consists primarily of Mesozoic intermediate calc-alkaline plutons with subordinate metamorphic complexes and basaltic to andesitic volcanic rocks (Zeil, 1986; Thornburg and Kulm, 1987a; Sernageomin, 2003). To the east of the Coastal Range, a forearc alluvial basin is filled with massive continental clastic and volcanoclastic rocks, which originate from the Andes (Thornburg and Kulm, 1987a). The volcanic arc itself is characterized by primarily andesitic ignimbrites (pre-Pliocene) that are overlain by Plio–Quaternary volcanoes. The volcanoes consist of andesitic rocks and tephra and reach elevations of more than 6000 m (Sernageomin, 2003).

From 27.5°S to 33°S Plio-Quaternary volcanism as well as alluvial forearc basins are absent, due to the low angle of the subduction zone in this region (Jordan and Gardeweg, 1989), and the area is characterized by a rather constant increase in elevation from the coast up to the Andes (Fig. 1). In this segment the Andes are characterized by more abundant plutons, as well as older sedimentary units, volcanic rocks, and outcrops of the metamorphic basement (Zeil, 1986). The elevation of this part of the cordillera is high; reaching maximum values of up to 7000 m asl around 33°S.

South of 33°S, both geology and geomorphology change abruptly (Lowrie and Hey, 1981) as the dip of the subduction zone increases again, and Plio–Quaternary volcanism and forearc alluvial basins reappear. The elevations of the Coastal Range (average maxima 1500 m asl) and, especially, of the Andes decrease substantially. The latter reveals a gradual average crestal elevation decrease from about 5000 m at 33°S to only 2000 m at 42°S (Scholl et al., 1970).

The geology of the Coastal Range south of 33°S is marked by abundant, primarily low-grade metamorphic rocks (Sernageomin, 2003), with Palaeozoic plutons also being common southwards to about 38°S (Sernageomin, 2003). The Chilean Central Depression is filled with up to 4000-m-thick sequences of alluvial sediments (Zeil, 1986). South of 41°S it has been invaded by the sea. Further east, the basement of the Andes consists mainly of Mesozoic plutons south of 41°S, in contrast to the pre-Pliocene andesitic volcanics and sediments that outcrop further north between 33°S and 41°S (Sernageomin, 2003). The Plio–Quaternary volcanics occurring throughout this Andean segment are more basic in chemistry than in northern Chile (Thornburg and Kulm, 1987a).

The precipitation gradient is opposite to the topographic one; rainfall rates rapidly increase from the extremely arid North to the South, ranging from close to zero in the core of the hyper arid Atacama Desert (~23°S) over intermediate values in the Mediterranean-type climate of central Chile (~33–37°S) to year-round humid conditions with extraordinary high annual precipitation values of up to 7500 mm/a south of 42°S (Miller, 1976) (Fig. 1). The extremely arid Atacama Desert in the North is a "rain-shadow" and a "cold-air" desert (Rauh, 1983) due to the combined effects of a high-pressure system located on the western Pacific Ocean, the drying effect of the cold north-flowing Peru–Chile current, and the rain-shadow effect of the Andes intercepting precipitation from the East (e.g., Arroyo et al., 1988; Fig. 2). Moreover, the Atacama Desert lies well north of the winter cyclonic precipitation (Southern Westerlies) that starts south of 25°S and is common south of 30°S (e.g., Messerli et al., 1993).

Although glaciers are present throughout the whole mountain range from ~17°S down to 55°S, due to the north–south temperature and precipitation gradients there is a strong increase in glacier occurrence going from the 'dry Andes' (~17°30–35°S) to the 'wet Andes' (>35°S, Iliboutry, 1999), leading to increased glacier-induced erosion (or denudation) rates towards the South.

Since initial studies by Scholl et al. (1970), it has been known that the amount of terrigenous sediment supplied to the Chilean margin over the Late Cenozoic is strongly related to onshore rainfall. Analyses of sediment cores from the Chilean continental slope for palaeo-environmental studies revealed that a similar pattern can also be found in more recent sedimentation rates (Hebbeln et al., 2000). These studies show that Holocene sedimentation rates off arid northern Chile are on the order of a few centimetres per ka, increasing to extremely high values of more than 100 cm/ka off southern Chile. Off southern Chile the remarkably high sedimentation rates even lead to the complete burial of the structural trench south of 38°S (Fig. 1).

Sedimentological studies on the Chilean continental margin that relate sediment composition to provenance are rather scarce. Krissek et al. (1980) and Scheidegger and Krissek (1982), studied a set of surface sediments from the Nazca Plate and the Peru–Chile continental margin just north of 25°S and used bulk chemistry, mineralogy, and texture of the terrigenous sediment fraction to evaluate the factors influencing sediment formation. In the same area, Rosato and Kulm (1981) used the clay mineralogy to infer provenance, sea-level changes, and continental accretion. Thornburg and Kulm (1987a, b) focused on sands in the Chile Trench and gave a general petrofacies classification of the Peru–Chile trench sediments. Lamy et al. (1998) were the first to present a study of the grain-size distributions (terrigenous silts, 2–63 μm), bulk mineralogy, and clay mineralogy of a set ($N = 48$) of surface samples from the Chilean continental slope. They concluded that regional variations in silt size and bulk mineralogy are governed by the source–rock composition of the different geological terranes and the relative source–rock contribution of the Coastal Range and Andes, as controlled by the continental hydrology. These results were later complemented by bulk chemistry analyses of the same set of surface samples (Klump et al., 2000).

The regional oceanography of the Southeast Pacific was summarised by Strub et al. (1998) and its impact on the sediment distribution, with emphasis on the oceanic primary production, was described by Hebbeln et al. (2000). The latter study revealed also for the

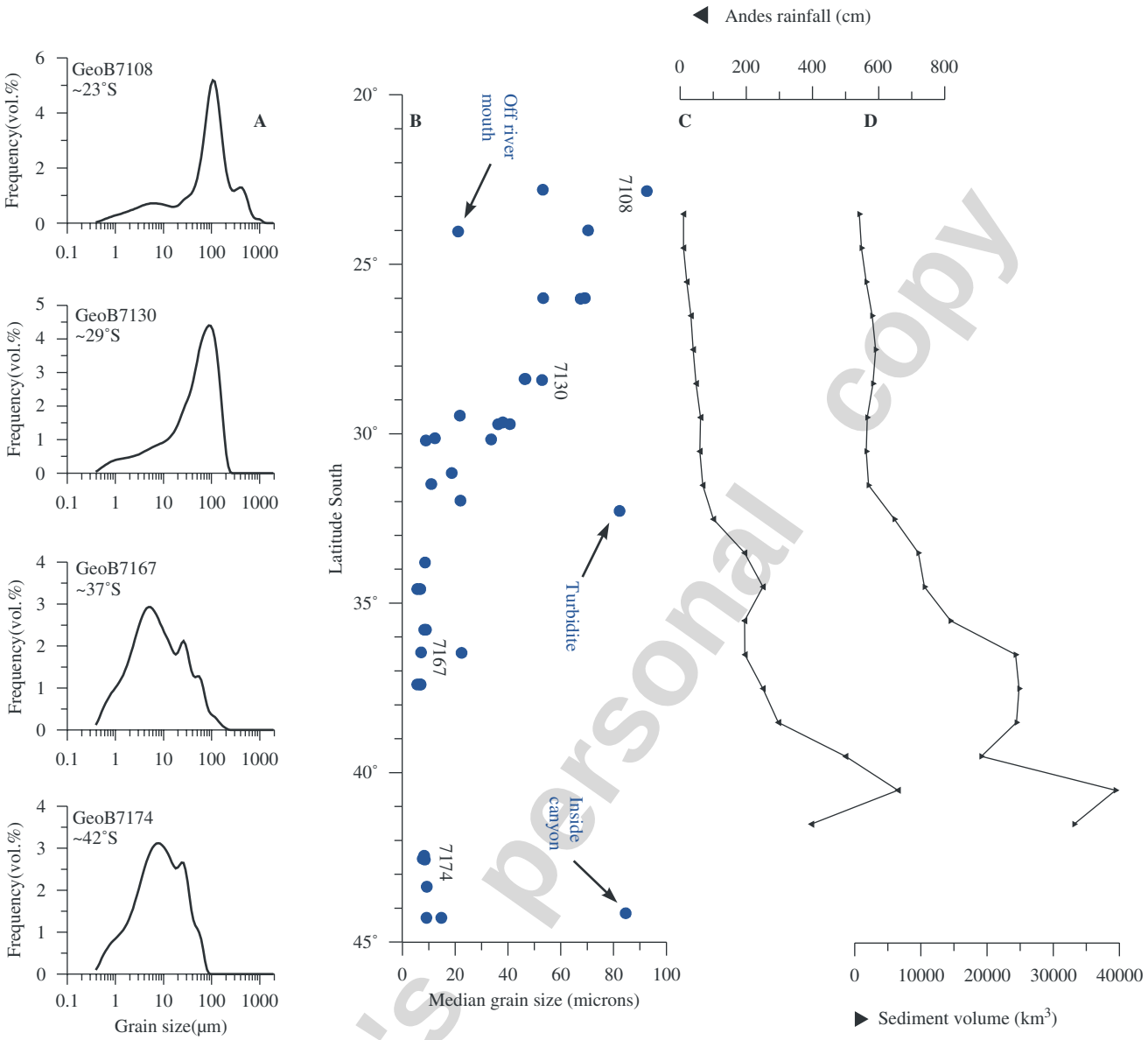

Fig. 2. Grain-size distributions of the terrigenous sediment fraction in relation with climate: (a) typical grain-size distributions of the terrigenous sediment fraction illustrating the mixture of land-derived sediments found on the continental slope ranging from predominantly wind-blown in the arid North to fluvial sediments in the humid South. GeoB71xx denotes samples, plotted also in B, (b) median grain size versus latitudinal position, (c) yearly precipitation plotted versus latitude (after Scholl et al., 1970) and (d) estimated total Cenozoic sediment volume on the Chilean continental margin plotted versus latitude (after Scholl et al., 1970).

accumulation of the biogenic sediment compounds a strong southward increase that reaches even beyond the southern limit of the Chilean coastal upwelling area at ~39°S. However, despite the high fertility of the Peru–Chile Current, the contribution of biogenic material to the Chilean slope sediments is always below 20% due to the considerable input of terrigenous sediments (Hebbeln et al., 2000).

The aim of this study is to provide a comprehensive new data set ($N = 70$) of the surface sediment composition along the Chilean continental slope between 23–44°S. Furthermore, the observed variation in physical, chemical and mineralogical properties of the terrigenous sediment fraction from the Chilean continental slope can be used to deduce variations in sediment transport mechanisms and sediment provenance.

2. Material and methods

The study area stretches from about 23°S to about 44°S along the Chilean continental margin in the Southeast Pacific Ocean (Fig. 1). All samples were taken by a multicorer from the continental shelf and slope in several slope-normal transects from water depths varying from 122 to 4467 m bsl (Table 1, Fig. 1) during expedition SO156 with the German RV Sonne (Hebbeln et al., 2001). From

Table 1
Position and water depth of the surface samples ($N = 70$) presented in this study

Sample	Lat (°S)	Lon (°W)	Depth (m)	Sample	Lat (°S)	Lon (°W)	Depth (m)
7103-4	22°52.03	70°32.53	890	7154-2	33°47.99	72°16.49	1385
7104-6	22°52.00	70°29.42	312	7155-1	34°34.99	72°53.21	2746
7106-1	22°48.02	70°36.71	1351	7156-1	34°35.04	72°30.61	1247
7108-1	22°50.50	70°34.81	1006	7157-1	35°46.99	73°35.32	2107
7112-1	24°01.99	70°49.42	2508	7158-1	35°47.00	73°28.54	1563
7114-1	23°59.98	70°49.92	1395	7159-1	35°47.00	73°13.60	506
7115-1	23°59.99	70°35.71	523	7160-4	36°02.31	73°04.41	366
7116-1	26°00.01	70°59.99	1996	7161-5	36°25.54	73°23.31	126
7118-1	25°59.98	70°48.55	460	7162-4	36°32.56	73°40.03	798
7119-1	26°00.00	70°52.08	954	7163-5	36°25.53	73°35.78	539
7120-1	26°01.08	71°14.19	4467	7167-4	36°27.15	73°54.49	2064
7121-1	25°59.97	70°54.09	1442	7169-2	37°23.99	74°19.00	3249
7122-1	25°59.99	70°50.42	673	7170-1	37°23.99	74°08.61	2229
7123-1	27°17.13	71°03.07	557	7171-2	37°23.96	73°57.13	1386
7127-1	28°23.02	71°28.27	1462	7174-3	42°32.64	75°00.08	1222
7129-1	28°25.01	71°19.80	476	7175-4	42°27.14	75°12.62	1967
7130-1	28°24.97	71°36.78	2080	7177-3	42°34.93	74°50.25	909
7131-1	28°23.00	71°30.10	1650	7179-1	42°34.01	75°20.19	2760
7132-1	29°27.99	71°53.58	3253	7181-1	43°22.02	75°16.54	1212
7133-1	29°22.58	71°38.55	635	7182-1	43°22.06	74°55.14	301
7134-1	29°43.14	71°46.44	1888	7183-1	44°03.41	75°07.78	443
7136-1	29°43.00	72°09.99	3189	7186-1	44°09.00	75°09.52	1171
7137-1	30°10.02	71°43.95	1199	7187-1	44°11.99	75°10.45	476
7138-1	30°07.99	71°52.17	2733	7189-1	44°17.00	75°23.42	868
7139-1	30°12.02	71°58.99	3267	7190-1	44°17.05	75°51.88	3285
7140-1	31°01.75	71°45.00	345	7191-1	44°16.99	75°35.55	1939
7141-1	31°05.34	71°44.99	301	7194-1	41°25.05	74°26.02	308
7142-1	31°10.78	71°45.00	481	7195-1	41°12.46	74°24.59	521
7144-1	31°09.62	71°58.12	1961	7197-1	40°59.99	74°33.00	816
7147-1	31°58.50	71°40.34	398	7212-1	39°41.75	74°22.67	1469
7148-1	31°58.49	71°55.87	2289	7213-1	39°43.88	74°17.22	1190
7149-1	31°29.14	72°00.01	3086	7215-1	39°48.99	74°03.96	498
7150-1	32°16.77	71°57.13	1591	7216-1	40°02.57	73°56.24	165
7152-1	33°48.00	72°06.61	420	7218-1	39°54.86	73°52.96	638
7153-1	33°47.98	72°09.62	863	7219-1	39°49.28	73°34.52	122

Note that both for the chemical and grain-size analyses, trends were only described for the samples from water depths > 1000 m.

the undisturbed surface sediment samples the uppermost centimetre has been used for the analyses reported here.

Grain-size analyses were performed on the bulk as well as the terrigenous ($C_{organic}$, $CaCO_3$, and Opal-free, after treatments with 10% HCl, 10% H_2O_2, and 1N NaOH, respectively) sediment fractions using a Coulter LS200 laser particle sizer, which resulted in grain-size distributions from 0.4 to 2000 μm in 92 size classes. It appeared that the shallow samples (<1000 m water depth, $N = 21$) show peculiar results, which are probably caused by reworking processes on the shelf and the upper slope. To ensure that the observed variations can reliably be related to sediment transport processes, we chose to consider only samples coming from water depths >1000 m.

Bulk chemistry was determined in two ways: seven major elements (K, Ca, Ti, Mn, Fe, Cu, and Sr) were determined by X-Ray Fluorescence Spectroscopy (XRF) in all surface samples using a non-destructive XRF core logging system especially developed for marine sediments. The general method and its applications are described by Jansen et al. (1998) and Röhl and Abrams (2000). Resulting element data are relative concentrations given in counts per second. Besides, element analyses were also carried out using total acid digestion and subsequent inductively coupled plasma atomic emission spectrometry (Perkin Elmer, Optima 3300RL), following the procedure described in Zabel et al. (2001).

To supplement the data set of terrigenous-sediment provenance proxies, we also include selected bulk- and clay-mineralogy data from the earlier study by Lamy et al. (1998). Methodological details related to these data can be found in Lamy et al. (1998).

3. Results

Nearly all grain-size distributions show a multimodal pattern, probably caused by the fact that these sediments are the result of mixing of different sediment populations related to different sediment transport mechanisms. Four characteristic grain-size distributions of the surface

sediments are shown in Fig. 2A, their latitudinal position indicated in Fig. 2B. Despite the fact that most distributions are multimodal, it is clear that wind-blown transport processes prevail in the North, leading to a relatively coarse mode (up to 100 μm, e.g., samples GeoB7108 and GeoB7130) in the grain-size distributions, whereas further south, the mean modal size is much finer grained (about 4–8 μm, e.g., samples GeoB7167 and GeoB7174). The generalised pattern is reflected in the median grain size of the samples plotted along the north–south transect in Fig. 2B. A clear decrease can be observed from about 70 μm at 23°S down to about 10 μm at 34°S. The fact that the median grain size does not decrease further between 34°S and 44°S indicates that similar sedimentation processes may prevail along this relatively large latitudinal range. One exception to this trend showing a median grain size of about 25 μm at 23°S—indicated by an arrow in Fig. 2B—is located directly offshore an ephemeral river mouth. Two other exceptions to the trend showing a median grain size of >80 μm relatively far south—also indicated by arrows in Fig. 2B—are interpreted as the result of mass-flow deposits or turbidity currents (sample at about 32°S), and due to sediment focussing effects of a deep-marine canyon (sample at about 44°S), respectively.

Of the chemical data, mainly the contributions of iron (Fe), titanium (Ti), potassium (K), aluminium (Al), magnesium (Mg) and zirconium (Zr) allow inferences about the land-derived material. Various ratios of these elements show distinct latitudinal trends (Fig. 3) that allow a differentiation of four areas, with all of these being marked by individual element mixtures. The northernmost area (22.5–24.5°S) is marked by high Fe, and Ti contents, whereas Al, and K are very low. Between 25.5°S and 33°S this pattern is reversed with the most pronounced shift around 25°S. From there especially the Fe/K and Ti/K ratio show a continuous increasing trend even as far south as 36°S. From 33°S to 40°S high Al and Zr contributions are complemented by high Fe and Ti values and low to intermediate K and Mg values. Finally, in the southernmost sector (40–45°S) the most obvious changes are related to a relative increase in Mg and K.

The mineralogical data from Lamy et al. (1998) show a large variability within the individual transects but nevertheless reveal some general patterns (e.g., in the quarz/feldspar and illite/chlorite ratios shown in Fig. 3). Both ratios show highest values and largest scatter between 25°S and 32°S (the region north of 25°S is not covered by this data set). Towards the south, around 42°S, the quartz/feldspar ratio continues to decrease, whereas the illite/chlorite ratio is marked by a slight increase compared to the lowest values around 35°S.

To summarise the results from grain size, chemistry and mineralogy, selected data are presented in ternary diagrams in Fig. 4, to illustrate the above-mentioned trends. All data are grouped into three latitudinal bands, and all data sets are restricted to the samples from water depths >1000 m.

4. Discussion

The large latitudinal rainfall gradients in Chile on one hand and the variable Chilean geology on the other hand are expected to leave their imprint in the marine sediments deposited along the Chilean continental slope, both in terms of texture and composition. Especially, the distinct precipitation pattern certainly affects the sediment transport processes. Terrigenous sediments deposited off the arid northern part of Chile are likely predominantly wind blown, whereas further south under more humid conditions, terrigenous sediments are most probably river transported. In studies carried out in different sedimentary basins and settings it was shown that different sediment-transport processes leave a typical imprint on the grain-size distributions of the terrigenous sediment fraction (Prins and Weltje, 1999; Stuut et al., 2002; Weltje and Prins, 2003; Frenz et al., 2004; Holz et al., 2004; Stuut et al., 2005). In the sediments deposited on the Chilean continental slope, the observed dominant grain-size patterns are related mainly to the sediment-transport mechanisms that brought the sediments there. However, due to the large topographic gradients, there is a large amount of rivers discharging onto the continental margin, leading to a very heterogeneous mixture of sediments originating from a multitude of small rivers. To exclude disturbances caused by reworking processes on the shelf, and in order to bias the results towards potentially sediment-transport driven, we chose to discuss only the samples that came from water depths >1000 m. Despite that, geomorphological features like e.g., canyon incisions now and then cause anomalous results (Fig. 2). Furthermore, since the Chilean continental margin is located on an active subduction zone, earthquake-driven mass-flow deposits occur as well, which are represented for example by the very coarse-grained sample at ~32°S (Fig. 2). Further anomalous grain-size distributions have been observed, which contained large fragments of volcanic glass, indicating that volcanism is an additional source of terrigenous particles in the study area. However, despite all these potential disturbances, some general trends can be observed. The grain-size distributions that are shown in Fig. 2A, clearly show a multimodal character with one dominant mode. This mode can be ascribed to one particular sediment type, transported by a single dominant transport mechanism. In the North we suggest that this dominant mode is related to wind-blown dust from the Atacama Desert. Given the approximate source-to-sink distances the grain-size results compare very well with present-day dust collected from the atmosphere offshore the Saharan Desert (Stuut et al., 2005). The grain-size distribution of sample GeoB7130, collected at about 29°S shows a typical distribution that can be related to wind-blown transport: practically unimodal, well sorted, and with a median size of about 80 μm. Further South the modal size decreases dramatically from average 70 μm to average 6 μm towards 30°S, and stays more or less constant further South. We argue that South of 30°S, the mixture of

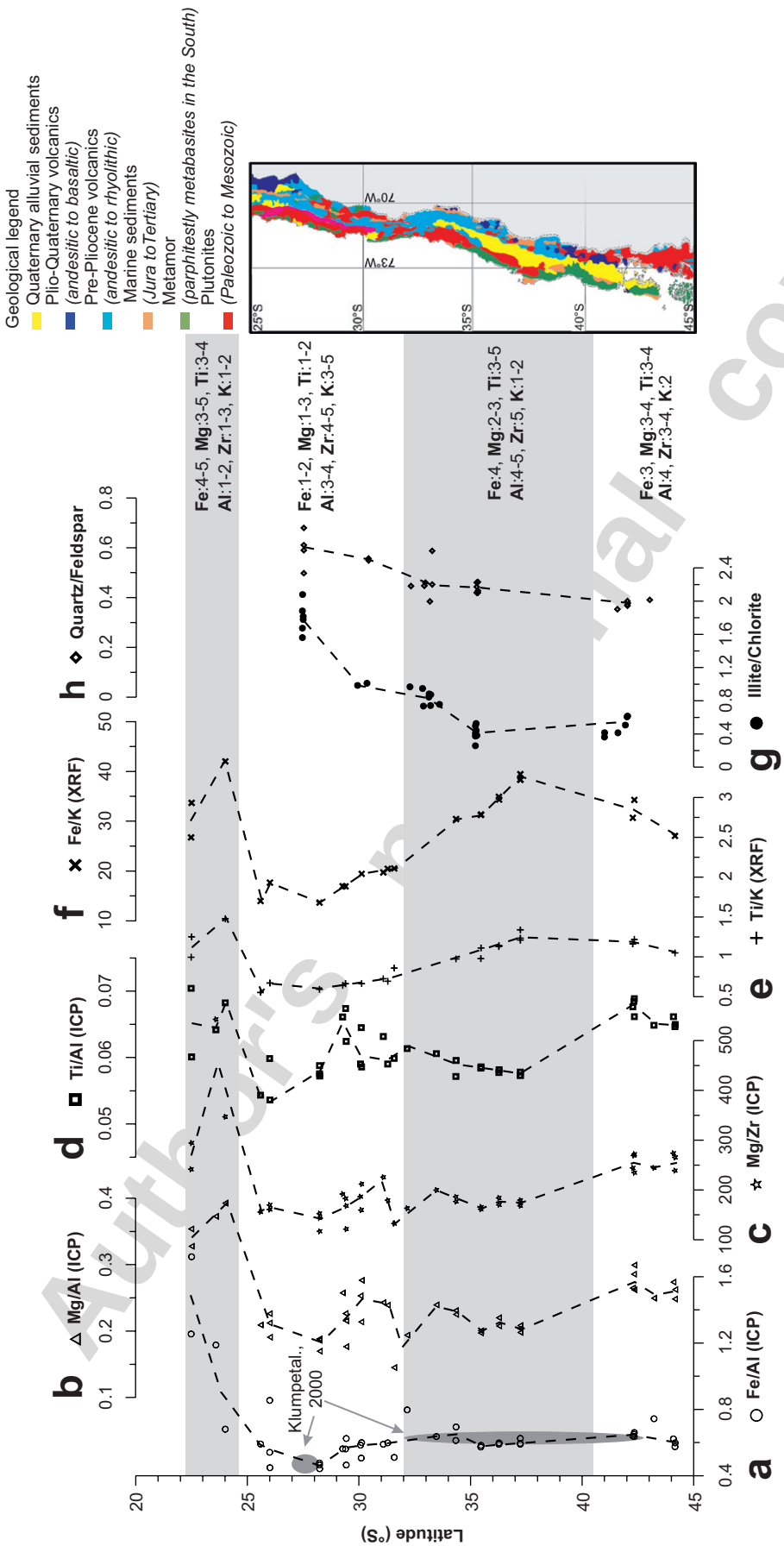

Fig. 3. Bulk chemical (ICP-MS and XRF) and mineralogical data vs. latitude and simplified geological map of the hinterland (simplified after Thornburg and Kulm, 1987a) Grey shadings roughly indicate simplified geological terranes on the continent: (a) Fe/Al ratio as measured by ICP (open dots). Rough Fe/Al values published by Klump et al. (2000) are indicated by shaded elipses, (b) Mg/Al ratio as measured by ICP (open triangles), (c) Mg/Zr ratio as measured by ICP (open squares), (d) Ti/Al ratio as measured by ICP (open stars), (e) Ti/K ratio as measured by XRF (+ signs), (f) Fe/K ratio as measured by XRF (x signs), (g) Illite/Chlorite ratio (filled dots, from Lamy et al., 1998) and (h) Quartz/Feldspar ratio (open diamonds, from Lamy et al., 1998).

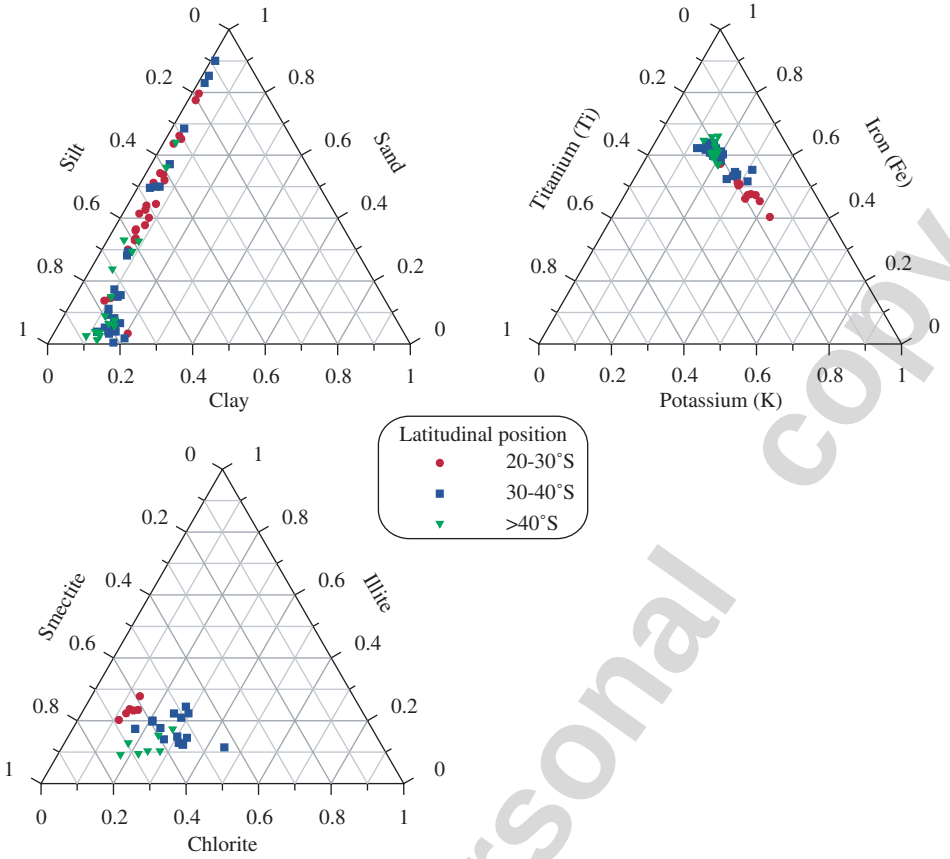

Fig. 4. Grain-size, bulk chemical and mineralogical data in ternary diagrams: (a) Median grain size plotted in a sand–silt–clay diagram, (b) Bulk chemistry (ICP-MS) results for the elements Iron (Fe), Titanium (Ti), and Potassium (K) and (c) Clay-mineralogical results for the minerals Illite, Smectite and Chlorite.

which the sediments is composed changes from wind-blown dominated to fluvial dominated. The dominant transport mode here is related to river-transported sediments from the numerous rivers that drain the Andes Mountains. Due to the heterogeneity within all these rivers in terms of average length, drainage area, and discharge, a considerable variability is to be expected in the modal size of the fluvial mud. However, when considering the samples collected South of 30°S, and from >1000 m water depth, this variability is surprisingly low; only a few microns (Fig. 2B). This observation supports the idea that fluvial mud in the deep sea can be characterised on the basis of its size of about mud to fine-silt with a modal size of 4–8 μm (e.g., Prins et al., 1999; Stuut et al., 2002).

It is striking that the north–south trend in the modal grain-size shows an apparent change in the sediments' texture at about 30°S (Fig. 2B), whereas the chemistry, especially the Fe/K ratios, (Fig. 3) indicates a major increasing trend from 32°S to 37°S. If the observed changes would be solely due to changes in the sediment transport mechanisms, they would have to occur at the same latitude. Given the predominantly wind-blown origin of the sediments in the North, one would expect relatively high iron values due to the iron-coated particles blown in from the Atacama Desert. However, the trend from North to South are relatively continuous Fe/Al and Ti/K ratios (Figs. 3A and E), which cannot be explained by an increase in relative amount of river sediments to the South, should one believe for example that the light elements Aluminum and Potassium are preferably transported in clay minerals.

In studies covering a latitudinal range from 27°S to 43°S (Lamy et al., 1998; Klump et al., 2000) it was suggested that the sediments off northern Chile primarily originate from the Coastal Range and are supplied by wind, which is consistent with the grain-size data presented here. Their data, shown as Fe/Al, quartz/feldspar, and illite/chlorite ratios in Fig. 3, agree well with the trends in the element compositions determined in this study. Between 25°S and 30°S the absence of larger rivers transporting material from the Andes to the coast results in mineralogical and elemental composition characteristics typical for a coastal range provenance. These include comparatively high amounts of quartz, illite, Al, and K, whereas feldspar, chlorite, Fe, and Ti are less common. These data are consistent with predominantly felsic plutonic source rocks with subordinate amounts of metamorphic rocks and basaltic to andesitic volcanic lithologies, and, thus, point to a predominantly Coastal Range provenance.

Interestingly, the new data from north of 25°S indicate this latitude as marking the most pronounced shift in the

composition of the terrigenous sediments. North of 25°S the sediments exhibit very high Fe/Al, Ti/Al, Fe/K, and Ti/K ratios. This elemental composition points to source rocks of very basic composition; most likely related to the volcanic rocks of the Andes. Comparison to the 25–30°S segment indicates a substantially higher Andean source rock contribution off northernmost Chile. Whereas most of the grain-size distributions in these regions are typical for prevailing aeolian input (as in the southward adjacent segment), there may nevertheless be a fluvial contribution as well (e.g. the "anomalous" sample of the river mouth). Indeed, rainfall at the crest of the Andes tends to increase again towards northernmost Chile, induced by summer rainfall originating from the Amazonas basin. This rainfall allows for a few rivers (e.g., Rio Loa) to cut through the Coastal Range and supply Andean material to the continental margin, which may consequently be distributed along the margin and not necessarily be clearly visible in all grain-size distributions. In addition and in contrast to the 27–33°S segment, Quaternary volcanic activity is present in the north, providing more abundant basic source rock material and volcanic ashes that may be likewise transported by aeolian transport processes to the ocean.

Further south (~>32°S) increased precipitation allows rivers originating from the Andes to cut through the Coastal Range and to supply Andean material, mostly basaltic-andesitic source rocks, to the continental slope. This Andean source is clearly reflected in higher plagioclase and pyroxene, less quartz, K-feldspar and mica contents and lower illite/chlorite ratios (see Lamy et al., 1998), as well as higher Fe/Al, Mg/Zr, and Ti/K ratios (Fig. 3). These mineralogical assemblages would be consistent with the observed pattern of higher relative contributions of Al, Zr, and K (and lower relative contributions of Fe, Mg, and Ti) derived from northern Chile between 25 and 32°S (Fe-poor source rocks, high amount of K-bearing minerals such as K-feldspar, illite, mica) and conversely higher Fe/Al, Mg/Zr, and Ti/K ratios to the south (>32°S) characteristic of the predominating Andean source. Although there is little variability in the Fe/Al and Mg/Zr ratios between 32 and 40°S, the Ti/K ratio continuously increases to maximum values at ~38°S, possibly reflecting the southward increasing supply of andesitic to basaltic Plio–Quaternary volcanics from the Andes (Fig. 3E). In addition, this increase may also reflect the southward trend in the composition of the volcanic arc that becomes clearly more basic towards the south (Hildreth and Moorbath, 1988; Stern, 2004).

The shift from primarily Andean to Coastal Range provenance was earlier suggested to be located around 33°S (Lamy et al., 1998, Klump et al., 2000), and which is still consistent with our new data based on a denser network of surface samples. However, the data presented here indicate a more gradual shift between ~32°S and 37°S (Fig. 3). It is striking that this shift in source rock contribution occurs a few degrees further south than the shift in the mode of sediment transport (aeolian vs. fluvial) at ~30°S. If the observed changes would be solely due to changes in the sediment transport mechanisms, they would have to occur at the same latitude. However, the observed offset implies that the rivers between ~30°S and 33°S primarily supply Coastal Range material, and only further south provide substantial material originating from the Andes.

The southward increase of the Fe/K ratio can be explained taking the onshore source–rock geology into account; In the north (north of 33°S) there are mainly Mesozoic intermediate calc-alkaline plutons with subordinate metamorphic complexes and basaltic to andesitic volcanic rocks (Zeil, 1986; Thornburg and Kulm, 1987a), which are poor in iron. South of 33°S, there are mainly andesitic volcanic rocks, changing to predominantly plutonic rocks from about 39°S southwards that are relatively enriched in iron.

A similar north–south trend is observed in the clay minerals, although the northernmost (Atacama, predominantly wind-blown) samples are not all clearly distinguished from those further South. The increase in smectite contents becomes more evident going further South (Fig. 4C). The change from illite to smectite can be interpreted as a change from physical to chemical weathering, caused by the existing precipitation gradients; in the North weathering is predominantly physical changing to more chemical towards the South.

5. Conclusions

The combination of source–rock geology and sedimentation processes determine the composition and quantity of terrigenous sediments on the Chilean continental slope. Sediment-transport processes are essentially driven by climate; precipitation patterns govern runoff rates of the rivers draining the Andes Mountains, whereas sediment transport in the Atacama Desert is restricted to wind-blown transport. Based on this study of surface sediments we conclude that especially in the region of the most pronounced changes-approximately between 30°S and 35°S—grain size as well as bulk chemistry can be used to trace changes in provenance and climate-related sediment transport. Thus, the deep-sea sediments on the Chilean continental margin in this area of strong latitudinal precipitation gradients potentially contains an archive of paleoenvironmental changes that occurred throughout the past, and which can be reconstructed based on grain size and bulk chemistry (see e.g. Lamy et al., 1998).

Acknowledgements

We thank the crew and scientists aboard R.V. *Sonne* (Sonne cruise 156) for their help with coring and sampling operations. We also thank S. Röber (Bremen University) for carrying out the total acid digestions and ICP-AES analyses. The manuscript benefited strongly from the suggestions by M. Pino, D. Ariztegui, and an anonymous reviewer. Financial support was provided by the Deutsche Forschungsgemeinschaft as part of the DFG-Research

Center 'Ocean Margins' of the University of Bremen. This is publication No. RCOM0401.

References

Allmendinger, R.W., Jordan, T.E., Kay, S.M., Isacks, B.L., 1997. The evolution of the Altiplano-Puna Plateau of the Central Andes. Annual Review Earth and Planetary Sciences 25, 139–174.

Arroyo, M.T.K., Squeo, F.A., Armesto, J.J., Villagrán, C., 1988. Effects of aridity on plant diversity in the Northern Chilean Andes: results of a natural experiment. Annals of the Missouri Botanical Garden 75 (1), 55–78.

Frenz, M., Höppner, R., Stuut, J.-B.W., Wagner, T., Henrich, R., 2004. Surface sediment bulk geochemistry and grain-size composition related to the oceanic circulation along the South American continental margin in the Southwest Atlantic. In: Wefer, G., Mulitza, S., Ratmeyer, V. (Eds.), The South Atlantic in the Late Quaternary-Reconstruction of Material Budgets and Current Systems. Springer, Berlin, pp. 347–373.

Hebbeln, D., and cruise participants, 2001. PUCK: report and preliminary results of R/V Sonne Cruise SO 156, Valparaiso (Chile)—Talcahuano (Chile), March 29—May 14, 2001. Berichte aus dem Fachbereich Geowissenschaften der Universität Bremen vol. 182. Bremen University, Bremen, p. 195.

Hebbeln, D., Marchant, M., Freudenthal, T., Wefer, G., 2000. Surface sediment distribution along the Chilean continental slope related to upwelling and productivity. Marine Geology 164 (3–4), 119–137.

Hildreth, W., Moorbath, S., 1988. Crustal contributions to arc magmatism in the Andes of central Chile. Contributions to Mineralogy and Petrology 98, 455–489.

Holz, C., Stuut, J.-B.W., Henrich, R., 2004. Terrigenous sedimentation processes along the continental margin off NW-Africa: implications from grain-size analyses of surface sediments. Sedimentology 51 (5), 1145–1154.

Iliboutry, L., 1999. Glaciers of Chile and Argentina. In: Williams, R.S., Ferrigno, J.G. (Eds.), Satellite image atlas of glaciers of the world. United States Geological Survey Professional Paper 1386-I, 〈http://pubs.usgs.gov/prof/p1386i/〉.

Jansen, J.H.F., Van der Gaast, S.J., Koster, B., Vaars, A.J., 1998. CORTEX, a shipboard XRF-scanner for element analyses in split sediment cores. Marine Geology 151 (1–4), 143–153.

Jordan, T.E., Gardeweg, P.M., 1989. Tectonic evolution of the late Cenozoic central Andes (20°–33°S). In: Ben-Avraham, Z. (Ed.), The Evolution of the Pacific Ocean Margins. Oxford University Press, New York, pp. 193–207.

Klump, J., Hebbeln, D., Wefer, G., 2000. The impact of sediment provenance on barium-based productivity estimates. Marine Geology 169, 259.

Krissek, L.A., Scheidegger, K.F., Kulm, L.D., 1980. Surface sediments of the Peru-Chile continental margin and the Nazca plate. Geological Society of America Bulletin, Part 1 91, 321–331.

Lamy, F., Hebbeln, D., Wefer, G., 1998. Terrigenous sediment supply along the Chilean continental margin: modern regional patterns of texture and composition. Geologische Rundschau 87, 477–494.

Lowrie, A., Hey, R., 1981. Geological and geophysical variations along the western margin of Chile near lat 33° to 36°S and their relation to Nazca plate subduction. Geological Society of America Memoir 154, 741–754.

Messerli, B., Grosjean, M., Bonani, G., Burgi, A., Geyh, M.A., Graf, K., Ramseyer, K., Romero, H., Schotterer, U., Vuille, M., 1993. Climate change and natural resource dynamics of the Atacama altiplano during the last 18,000 years: a preliminary synthesis. Mountain Research and Development 13 (2), 117–127.

Miller, A., 1976. The climate of Chile. In: Schwerdtfeger, W. (Ed.), World Survey of Climatology, vol. 12. Elsevier, Amsterdam, pp. 113–145.

New, M., Todd, M., Hulme, M., Jones, P., 2001. Precipitation measurements and trends in the twentieth century. International Journal of Climatology 21, 1899–1922.

Prins, M.A., Weltje, G.J., 1999. End-member modeling of siliciclastic grain-size distributions: the Late Quaternary record of eolian and fluvial sediment supply to the Arabian Sea and its paleoclimatic significance. In: Harbaugh, J.W., Watney, W.L., Rankey, E.C. (Eds.), Numerical Experiments in Stratigraphy: Recent Advances in Stratigraphic and Sedimentologic Computer Simulations. SEPM Special Publication 62. Society for Sedimentary Geology, Tulsa, pp. 91–111.

Prins, M.A., Stuut, J.-B.W., Lamy, F., Weltje, G.J., 1999. End-member modelling of grain-size distributions of deep-sea detrital sediments and its palaeoclimatic significance: examples from the NW Indian, E Atlantic and SE Pacific Oceans. Geophysical Research Abstracts 1, 564.

Rauh, W., 1983. The Peruvian-Chilean deserts. In: West, N.E. (Ed.), Temperate Desert and Semi-deserts. Ecosystems of the World, vol. 5. Temperate Deserts and Semi-deserts. Elsevier, Amsterdam, pp. 239–267.

Röhl, U., Abrams, L.J., 2000. High-resolution, downhole, and nondestructive core measurements from sites 999 and 1001 in the Caribbean Sea: application to the late paleocene thermal maximum. In: Leckie, R.M., Sigurdsson, H., Acton, G.D., Draper, G. (Eds.), Proceedings of the ODP. Scientific Results, pp. 191–203.

Rosato, V.J., Kulm, L.D., 1981. Clay mineralogy of the Peru continental margin and adjacent Nazca plate: implications for provenance, sea level changes, and continental accretion. Geological Society of America Memoir 154, 545–568.

Ruiz, C., Corvalan, J., 1968. Mapa Geologico de Chile Scale 1:1,000,000. Santiago Instituto de Investigaciones Geologicas, Santiago, Chile.

Scheidegger, K.F., Krissek, L.A., 1982. Dispersal and deposition of eolian and fluvial sediments off Peru and northern Chile. Geological Society of America Bulletin 93, 150–162.

Scholl, D.W., Christensen, M.N., Von Huene, R., Marlow, M.S., 1970. Peru-Chile Trench. Sediments and sea-floor spreading. Geological Society of America Bulletin 81, 1339–1360.

Sernageomin, 2003. Mapa Geológico de Chile: versión digital. Servicio Nacional de Geología y Minería, Publicación Geológica Digital, No. 4 (CD-ROM, versión1.0, 2003). Santiago.

Stern, C.R., 2004. Active Andean volcanism: its geologic and tectonic setting. Revista geologica Chile 31 (2), 161–206.

Strub, P.T., Mesias, J.M., Montecino, V., Rutllant, J., Salinas, S., 1998. Coastal ocean circulation off western South America. In: Robinson, A.R., Brink, K.H. (Eds.), The Global Coastal Ocean—Regional Studies and Synthesis. Wiley, New York, pp. 273–313.

Stuut, J.-B.W., Prins, M.A., Schneider, R.R., Weltje, G.J., Jansen, J.H.F., Postma, G., 2002. A 300-kyr record of aridity and wind strength in southwestern Africa: inferences from grain-size distributions of sediments on Walvis Ridge, SE Atlantic. Marine Geology 180, 221–233.

Stuut, J.-B.W., Zabel, M., Schefuss, E., Ratmeyer, V., Helmke, P., Lavik, G., Schneider, R., 2005. Provenance of present-day eolian dust collected off NW Africa. Journal of Geophysical Research 110 (D04202), 14.

Thornburg, T., Kulm, L.D., 1987a. Sedimentation in the Chile Trench: petrofacies and provenance. Journal of Sedimentary Petrology 57 (1), 55–74.

Thornburg, T.M., Kulm, L.D., 1987b. Sedimentation in the Chile Trench: depositional morphologies, lithofacies and stratigraphy. Geological Society of America Bulletin 98, 33–52.

Weltje, G.J., Prins, M.A., 2003. Muddled or mixed? Inferring palaeoclimate from size distributions of deep-sea clastics. Sedimentary Geology 162 (1), 39–62.

Zabel, M., Schneider, R.R., Wagner, T., Adegbie, A.T., DeVries, U., Kolonic, S., 2001. Late Quaternary climate changes in Central Africa as inferred from terrigenous input to the Niger Fan. Quaternary Research 56, 207–217.

Zeil, W., 1986. Südamerika. Geologie der Erde, 1. Enke Verlag, Stuttgart, 160 pp 〈http://www.pangaea.de〉.